Suppression of Adjacent-Channel, Cochannel, and Intersymbol Interference by Equalizers and Linear Combiners

Brent R. Petersen, *Member, IEEE,* and David D. Falconer, *Fellow, IEEE*

***Abstract*— We describe the ability of a linear equalizer/combiner or decision-feedback equalizer to suppress all received adjacent-channel, intersymbol, and cochannel interference. The emphasis is on values among transmitter bandwidth, receiver bandwidth, carrier spacing, and antenna diversity which provide the best opportunities for interference suppression. Through analyses of the number of degrees of freedom and constraints in generalized zero-forcing equalizers, and partial comparisons to calculations of equalizer minimum-mean-square performance, four results are obtained. First, with one antenna and a linear equalizer, arbitrarily large receiver bandwidths allow for marginal improvements in spectral efficiency through decreased carrier spacing, because the carrier spacing cannot be reduced to a value below the symbol rate without incurring unsuppressible interference. Second, large receiver bandwidths assist multiple antennas in improving the spectral efficiency in that carrier spacing values may go below the symbol rate, even in the presence of cochannel interference. Third, the use of equalizers and linear combiners, together with large receiver bandwidths, allows large transmitter bandwidths to be used. Fourth, for cochannel interference and intersymbol interference, the number of interferers that may be suppressible by a generalized zero-forcing linear equalizer/combiner increases linearly with the *product* of the number of antennas and the truncated integer ratio of the total bandwidth to the symbol rate.**

I. Introduction

Efficient use of the available bandwidth in communication systems requires methods such as crowding of frequency-division multiplexed signals, reusing frequencies in cellular systems, and increasing data rates [1], [2]. Use of these, or other methods, to improve spectral efficiency often leads to more adjacent-channel interference (ACI), cochannel interference (CCI), and intersymbol interference (ISI). ACI is the interference due to signals with different carrier frequencies which are close enough to cause mutual overlaps in the spectra. CCI is the interference due to signals with similar carrier frequencies. ISI is the interference among the data of interest. It is necessary to find efficient techniques to simultaneously reduce the harmful effects of ACI, CCI, and ISI in digital communication systems. The use of equalizers and linear combiners (antenna diversity) is shown to be such a technique.

This paper is concerned with the situation occurring when the signal carrying the data of interest (containing ISI) and the signals of the interferers (ACI and CCI) are linearly modulated by their respective data, where all systems use the same symbol rate, and where the receivers make decisions at that symbol rate. Therefore some of the analytical subtleties that arise in other continuous-time contexts do not arise here [3]. This means that our results, similar to our earlier results on CCI [4], turn out to lead to time-invariant receiver structures. Thus the interference suppression properties of equalizers and linear combiners that are reported in this paper are essentially based on the property that all symbol rates are similar. For convenience, denote this symbol rate by $1/T$.

In the situation with this type of interference, previous techniques to reduce the harmful effects of ACI, CCI, and ISI were done in a framework which did not employ all of the possibilities of interference presence, bandwidths, or antenna diversity. For example, using multiple antennas, postcursor ACI was subtracted from the received signal and the residual precursor ACI was treated as stationary noise [5]. For CCI, the interference suppression capabilities of multiple antennas were shown, without including the benefits of wide optimum combiner bandwidths relative to the symbol rate [6]. Work was reported which deals with ACI and ISI using T- to $T/5$-spaced equalizers [7], [8] without combined use of antenna diversity. A finite-complexity multidimensional decision-feedback equalizer (DFE) was used where estimates of the interference due to the two ACI signals were subtracted before the detector and the forward filter of the DFE suppresses the precursor ISI and ACI [9], assuming that the spectrum of the signals requires a guard band for every three signals. $T/2$-spaced optimum combiners were used to suppress ISI and CCI but not ACI [10]. However, the performance gains, through interference suppression, which have been obtained using antenna diversity have thus far not incorporated the beneficial effects of wide transmitter bandwidths with respect to the symbol rate [5], [6], [10].

To show the effectiveness of equalizers and linear combiners in suppressing ACI, CCI, and ISI we attempt to evaluate their performance in a framework which employs all of

Paper approved by M. J. Joindot, the Editor for Radio Communications of the IEEE Communications Society. Manuscript received February 26, 1992; revised May 11, 1993. This work was supported by the Cable Telecommunications Research Institute (CTRI), the Ontario Graduate Scholarship Program (OGS), and the Natural Sciences and Engineering Research Council (NSERC). This paper was presented in part at the First Virginia Tech Symposium on Wireless Personal Communications, Blacksburg, VA, June 3–5, 1991; the Third National Seminar and Workshop on Wireless Personal Communications, Calgary, Alberta, Canada, 1991; and the IEEE International Conference on Communications, Chicago, IL, June 14–18, 1992.

B. R. Petersen is with TR Labs., Calgary, Alberta T2L 2K7, Canada.

D. D. Falconer is with the Department of Systems and Computer Engineering, Carleton University, Ottawa, Ont. K1S 5B6, Canada.

IEEE Log Number 9406163.

the possibilities of interference presence, bandwidths, and antenna diversity. Two methods are used to evaluate the effectiveness of the equalizers/combiners. The first method is the *analysis* of the number of degrees of freedom and number of constraints for generalized zero-forcing linear and decision-feedback equalizers employing multiple antennas which try to suppress all ACI, CCI, and ISI. This analysis is based on the assumption that the values of the frequency responses of the channels give a system of linearly independent equations. The analysis is a generalization of the linear equalizer case of CCI and ISI with one antenna [4]. The second method is calculation of the minimum mean square error (MMSE) performance of continuous-time infinite-length linear and decision-feedback equalizers for the case of one antenna in a digital radio application.

Four results are obtained and presented in this paper. The results show some potential and limits of using frationally spaced equalizers and linear combiners to suppress ISI, ACI, and CCI. First, with one antenna and a linear equalizer, arbitrarily large receiver bandwidths allow for marginal improvements in spectral efficiency through decreased carrier spacing, because the carrier spacing cannot be reduced to a value below the symbol rate without incurring unsuppressible interference. Second, large receiver bandwidths assist multiple antennas in improving the spectral efficiency in that carrier spacing values may go below the symbol rate, even in the presence of CCI. Third, the use of equalizers and linear combiners, together with large receiver bandwidths, allows large transmitter bandwidths to be used. This may allow system design flexibility, e.g., constant or near-constant envelope modulation. Fourth, for CCI and ISI, the number of interferers that may be suppressible by a generalized zero-forcing linear equalizer/combiner increases linearly with the *product* of the number of antennas and the truncated integer ratio of the total bandwidth to the symbol rate.

For one antenna and no CCI, the interference suppression results of this analysis compare favorably with those offered by calculations of MMSE performance of linear and decision-feedback equalizers in a digital radio application. Calculations are not offered to further confirm the predictions of interference suppression in the multiple antennas case. Results are shown for *nonfading* channels, however, adaptive equalizers should also exhibit interference suppression capabilities for slowly varying channels. Although the carrier and symbol rates may differ, small differences would appear as slowly changing phase values which could be tracked by an adaptive equalizer.

This paper is organized as follows. Section I, the introduction, summarizes previous research and the contributions of this paper. Section II describes the model of the system. Section III contains the analysis of the number of degrees of freedom and constraints of a generalized zero-forcing linear equalizer/combiner and decision feedback equalizer in ISI, ACI, and CCI. Section IV contains a brief description of the expressions used to evaluate the minimum mean square performance of linear and decision-feedback equalizers. Section V contains the resutls of evaluations of regions where a generalized zero-forcing linear equalizer/combiner exists, as well as calculations of the minimum mean square performance of the equalizers for a digital radio application without fading. For the case of one receiver antenna, a *comparison* is included of the interference suppression capability of linear equalizers predicted by both the generalized zero-forcing analysis and the minimum mean square calculations. Finally, Section VI summarizes this paper.

II. System Model

The interference model with a continuous-time infinite-length linear equalizer receiver is shown in Fig. 1(a). A second situation considered in this paper occurs when the receiver in Fig. 1(b) replaces the receiver in Fig. 1(a); this is the situation of the same interference model with a continuous-time infinite-length decision-feedback equalizer. In this model define the impulse response of the *combined channel* to be $\phi_0(t)$, the convolution of both the pulse and the channel impulse responses. Define the impulse response of the ith *combined interferer* to be $\phi_i(t)$, the convolution of both the pulse and the interferer's transmission path impulse response. Since this model can represent a complex baseband system using linear modulation schemes, the interference can include both CCI and ACI. The signal component at the input to the receiver is given by

$$s(t) = \sum_{n=-\infty}^{\infty} d_0[n]\phi_0(t - nT) \tag{1}$$

where $d_0[n]$ are the transmitted data of interest and T is the symbol period. The noise plus interference (from L interferers) at the input to the receiver is given by

$$v(t) = n(t) + \sum_{i=1}^{L} \sum_{n=-\infty}^{\infty} d_i[n]\phi_i(t - nT) \tag{2}$$

where $n(t)$ is the complex white baseband noise and $d_i[n]$ are the data of the ith interferer. The term *cyclostationary interference* is used to describe $v(t)$ which consists of stationary noise and cyclostationary crosstalk. The input to the receiver is $g(t) = s(t) + v(t)$. The noise has a mean value of zero and a two-sided power spectral density of No. The data are mutually uncorrelated over the time index and the interferer number; the variance of the data is one.

III. Analysis—Generalized Zero-Forcing Equalizers

The discussion in this section develops results for linear equalizers/combiners and decision-feedback equalizers impaired by ISI, ACI, and CCI, which state that relatively wider bandwidths (with respect to the symbol rate) in the combined channel, combined interferers, and equalizer, may provide the flexibility to an equalizer/combiner to suppress larger numbers of interferers. This analysis also includes the effect of receiver antenna diversity. If the number of receiver antennas is A_r, it means that in Fig. 1(a) and 1(b) there are A_r times the number of combined channels and combined interferers and that receiver inputs are put together using a continuous-time infinite-length optimal combiner [5], [6], [10]. In other words, the output of each receiver antenna would be fed to a continuous-time infinite-length linear equalizer with

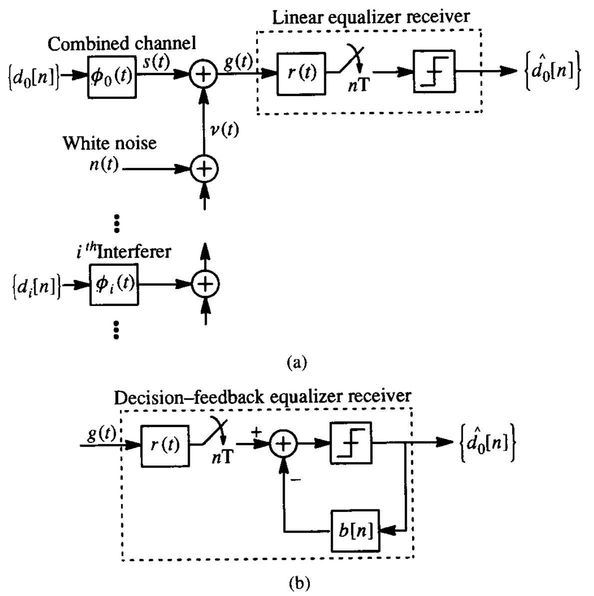

Fig. 1. (a) Continuous-time infinite-length linear equalizer in cyclostationary interference. (b) Continuous-time infinite-length decision-feedback equalizer.

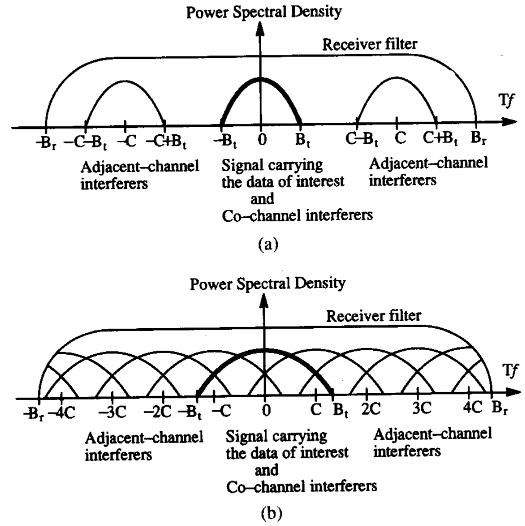

Fig. 2. (a) Magnitude response of the signals after receiver filtering—separated adjacent channels. (b) Magnitude response of the signals after receiver filtering—unseparated adjacent channels.

all equalizer outputs added together, and the adder output would be fed to the input of the quantizer. Note that the description of this result emphasized the work *may*; this is because wide relative bandwidths do not guarantee improved interference suppression capability under all conditions. Pathological conditions exist where wide relative bandwidths do not guarantee improved interference suppression, such as when the signal of interest and interferers have identical impulse responses. However, under conditions of linear independence, described later, wide relative bandwidths allow for substantial equalizer/combiner performance improvements over the case where narrow relative bandwidths are used, and the improvements are compounded by the use of multiple antennas. This linear independence is inherently demonstrated by the results in Section V, applied to digital radio systems.

In this generalization, the number of interferers L contains two components

$$L = N_a + N_c \tag{3}$$

where N_a is the number of ACI signals and N_c is the number of CCI signals present at the receiver input. Fig. 2(a) and 2(b) introduce three parameters. The transmitter bandwidth B_t equalizer/combiner (receiver) bandwidth B_r and carrier spacing C all of which are measured relative to the symbol rate, $1/T$. The figures also show the effect of the equalizer/combiner/receiver bandwidth. All signals are zero outside the frequency band $(-B_r/T,\ B_r/T)$. All the CCI signals have a carrier frequency of zero. However, although it is not shown in this paper, it would be a slight generalization to include multiple CCI signals at each carrier frequency. All the ACI carrier frequencies are separated by C/T with one ACI signal per carrier frequency. Depending on B_t, B_r, and C, a number of ACI signals may be present after receiver filtering. Fig. 2(a) shows a case where the adjacent bands are separated from the signal carrying the data of interest. In this particular case, the problem of ACI suppression is trivial; the receiver filter frequency response is set to zero in the adjacent interferers' bands. Of more interest in this paper is the situation shown in Fig. 2(b) where substantial spectral overlap occurs.

Define the *equalized combined channel* as

$$h_0(t) = \sum_{m=1}^{A_r} \phi_{0m}(t) \star r_m(t) \tag{4}$$

where the symbol $\star$ denotes convolution, $r_m(t)$ denotes the impulse response of the mth equalizer, $A_r \in \{1, 2, 3, \cdots\}$ is the number of antennas, and $\phi_{0m}(t)$ denotes the impulse response between the desired signal transmitter and the mth antenna element. Define the *equalized combined interferers* to be

$$h_i(t) = \sum_{m=1}^{A_r} \phi_{im}(t) \star r_m(t). \tag{5}$$

The time-domain condition for zero intersymbol interference at the sampling time can be written as

$$h_0(nT) = \begin{cases} 1, & n = 0 \\ 0, & n \neq 0 \end{cases} \tag{6}$$

and the time-domain condition for zero interference at the sampling time can be written as

$$h_i(nT) = 0; \qquad i \in \{1, 2, 3, \cdots, L\}. \tag{7}$$

The concept of suppressing interference by putting T-spaced zero crossings in the equalized combined interference responses is similar to the idea avoiding interference by generating nulls in an antenna pattern. A linear equalizer/combiner which causes (6) and (7) to be satisfied is called a *generalized zero-forcing linear equalizer* [11]. The analysis in this section is used to determine the conditions when such an equalizer/combiner is likely to exist in the ISI, ACI, and CCI model used. The fundamental premise of this section is that a generalized zero-forcing linear equalizer/combiner can exist if the number of degrees of freedom is less than or equal to the number of constraints. The combination of (6) and (7) also makes clear why all interfering signals should have the same symbol rate $1/T$.

Conditions (6) and (7) can be expressed in the frequency domain (using the normalized frequency ζ relative to $1/T$) as

$$\sum_{m=1}^{A_r}\sum_{i=-\infty}^{\infty}\Phi_{km}(\zeta+i)R_m(\zeta+i) = \begin{cases}1, & k=0\\ 0, & k=1,\,2,\,3,\cdots,L\end{cases} \quad (8)$$

where $\Phi_{km}(\zeta)$ is the Fourier transform of $\phi_{km}(t)$ for the mth antenna, and $R_m(\zeta)$ is the frequency response of the equalizer at the mth antenna output. This system of $L+1$ equations must be satisfied for any normalized frequency ζ. There is no loss of generality in taking ζ to be in the interval (0, 1). Because of finite receiver bandwidth, there are a finite number of nonzero terms in the sum over i. The equations in (8) can only be satisfied (and suppressing all ISI, ACI, and CCI) if for any frequency ζ, the number of unknowns $\{R_m(\zeta+i)\}$ equals or exceeds the number of equations $L+1$. In this section, we investigate the relationships between B_t, B_r, C, and A_r which allow such a solution. The system in (8) can also be expressed in matrix form, with obvious notation as

$$\underline{\boldsymbol{\Phi}}(\zeta)\underline{\boldsymbol{R}}(\zeta)=\underline{\boldsymbol{U}} \quad (9)$$

where

$$\underline{\boldsymbol{\Phi}}(\zeta) \triangleq [\Psi_1(\zeta)|\Psi_2(\zeta)|\Psi_3(\zeta)|\cdots|\Psi_{A_r}(\zeta)] \quad (10)$$

$$\underline{\boldsymbol{R}}(\zeta) \triangleq \begin{bmatrix}\underline{R}_1(\zeta)\\ \underline{R}_2(\zeta)\\ \vdots\\ \underline{R}_{A_r}(\zeta)\end{bmatrix} \quad \text{and} \quad \underline{\boldsymbol{U}} \triangleq \begin{bmatrix}1\\0\\ \vdots\\0\end{bmatrix} \quad (11)$$

$\underline{\boldsymbol{U}}$ has dimension $L+1$.

The elements of the submatrices $\Psi_m(\zeta)$ are $\Phi_{km}(\zeta+i)$, such that the number of rows in each matrix $\Psi_m(\zeta)$ is $L+1$, the total number of signal spectra within the receivers bandwidth B_r including that of the desired signal, CCI and ACI. The number of nonzero columns in each $\Psi_m(\zeta)$ (and of nonzero rows in $R_m(\zeta)$) is the number of indexes i, given ζ in (0, 1), for which the corresponding frequencies $\zeta+i$ are a) within the receiver's normalized frequency range $(-B_r,\, B_r)$, and b) values for which at least one of the $\{\Phi_{km}(\zeta+i)|k=0,1,\cdots,L,\, m=1,\,2,\cdots,A_r\}$ is nonzero.

Figs. 3–5 show ranges of (B_t, B_r, C, and A_r) for which feasible solutions exist. (These three figures are described in much more detail in Section V.) They are generated by varying B_t and C from 0 to 3, keeping B_r at one of B_t, $2B_t$, or $3B_t$, and keeping A_r at one of 1, 2, or 3. The number of ACI signals is not a parameter since exactly one ACI signal is assumed to be present, centered at every multiple of C relative to the desired signal. The number of ACI signals N_{ar} which interfere directly or indirectly with the signal of interest is

$$N_{ar}=\begin{cases}2\,\text{int}\left(\frac{B_t+B_r}{C}\right), & C\neq 0,\, C<2B_t\\ 0, & C\neq 0, C\geq 2B_t\end{cases} \quad (12)$$

where int (•) is the integer part of •.

In the definition of N_{ar}, *direct* ACI interferers spectrally overlap the desired signal; *indirect* ACI interferers are signals whose spectra overlap other direct or indirect interferers, but not the desired signal itself. For example, in Fig. 2(b) there are four direct ACI interferers and six indirect ACI interferers within the receiver's bandwidth. In this case $B_t \doteq 1.3C$, $B_r \doteq 3.3B_t$, and $N_{ar}=10$.

As well, in Fig. 5, one CCI signal is added (adding one to the number of equations). For each combination of parameters over a range of ζ, the nonzero terms in (8) are arrayed, and

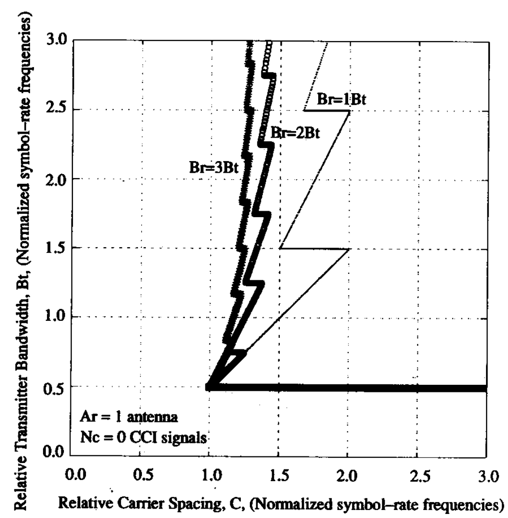

Fig. 3. Region of suppressible ISI, ACI, and CCI—Receiver bandwidth effects.

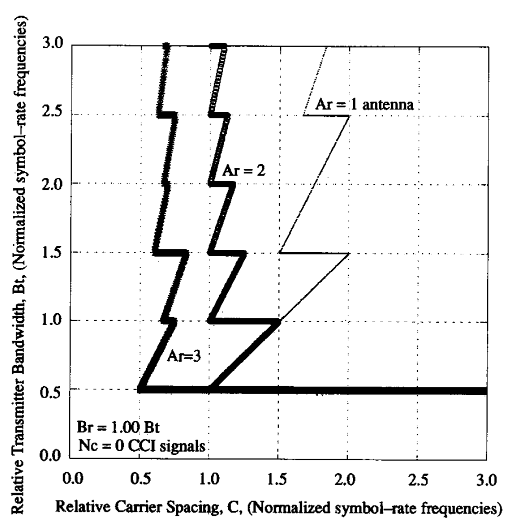

Fig. 4. Region of suppressible ISI, ACI, and CCI—Receiver antenna effects.

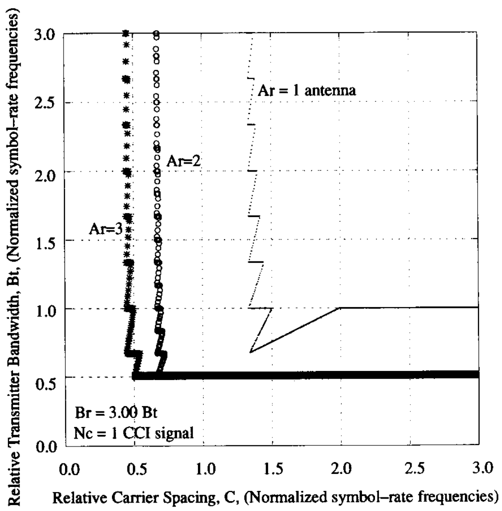

Fig. 5. Region of suppressible ISI, ACI, and CCI—Receiver antenna effects with one CCI signal and a wide receiver bandwidth.

the number of equations and unknowns is counted. A feasible solution is declared for a number of unknowns equal to or exceeding the number of equations.

Before the discussion, in section V, of the results shown in Figs. 3–5, we note that each of the submatrices $\Psi_m(\zeta)$ in (10) is assumed to have the same dimensions and to be linearly independent of all the other submatrices. These conditions imply that each of the impulse responses to A_r antennas are linearly independent and have similar bandwidths. Then the number of unknowns in (9) is a multiple of A_r, the number of antennas. For a fixed excess bandwidth relative to the symbol rate, if $L+1$, users can coexist (are separable) in the same band with a *single* antenna and equalizer, *then* $A_r(L+1)$ *users can coexist using* A_r *antennas and equalizers.*

Note too, that each *CCI signal* with the same bandwidth but with a different spectral shape from the desired and ACI signals, adds one more equation but no more unknowns, to the set of equations in (9), thus occasionally increasing the minimum carrier spacing C required for cancellation of ACI, CCI, and ISI signals with given bandwidth. The assumption of different spectral shapes for CCI and ACI signals corresponds to signals being received from different radio paths with different delays, carrier frequencies, and frequency responses.

This analysis also embodies the analysis for the case of no ACI, only ISI and CCI of [4]. In that case, it was shown that if the unnormalized transmitter and receiver bandwidths are $K/2T$, then up to K users can coexist. With A_r antennas, this number rises to A_rK. This result generalizes an earlier result in the literature which stated that with A_r antennas, A_r users can coexist [6]. *Our result indicates that the use of equalizers and linear combiners allows the number of suppressible interferers to increase linearly by the product of the number of antennas and system bandwidth relative to the symbol rate.*

Note that the foregoing analysis does not take into account the possibility of singularity in the matrix in (9). Thus, under the assumptions, it establishes *necessary* but not sufficient conditions for suppression of ISI, CCI, and ACI by a system of A_r antennas and A_r linear zero-forcing equalizers/combiners.

While this analysis is carried out for *linear* zero-forcing equalizers/combiners, it is equally applicable to zero-forcing DFE's when the linear equalizer in Fig. 1(a) is replaced by the decision-feedback equalizer in Fig. 1(b). The only difference to the appearance of the equations in (8) is that the 1 on the right-hand side is replaced by the discrete Fourier transform of the feedback tap coefficients

$$B_+(\zeta) = 1 + \sum_{k=1}^{\infty} b[k]e^{-j2\pi\zeta k/T} \tag{13}$$

where the + subscript indicates that only positive indices are allowed. $B_+(\zeta)$ constitutes one more unknown, and the system of equations in (9) changes to

$$[\underline{\boldsymbol{\Phi}}(\zeta) \mid -\underline{\boldsymbol{U}}] \left[\frac{\underline{\boldsymbol{R}}(\zeta)}{B_+(\zeta)}\right] = \underline{0} \tag{14}$$

where $\underline{0}$ is an $(L+1)$-dimensional vector of zeros. Equation (14) is a homogeneous set of linear equations and compared to (8) and it has one more unknown, although it is constrained to be of the form of (13). Thus, if it were to have a solution, one more interferer could be suppressed by a DFE than by a linear equalizer. It has a solution if the number of unknowns exceeds the number of equations (which is also true for a linear equalizer). If the number of unknowns, including $B_+(\zeta)$, *equals* the number of equations, $L+1$, it can have a nontrivial solution only if the determinant of the $(L+1)$ by $(L+1)$ matrix $\{\underline{\boldsymbol{\Phi}}(\zeta) \mid -\underline{\boldsymbol{U}}]$ is zero for all ζ. Unfortunately because of the form of $\underline{\boldsymbol{U}}$, this can only be true if the matrix formed by the last L rows and first L columns of $[\underline{\boldsymbol{\Phi}}(\zeta) \mid -\underline{\boldsymbol{U}}]$ has a zero determinant, for any ζ, which is not necessarily true. Thus, in general the DFE cannot suppress one extra interferer.

However, a DFE certainly gives extra degrees of freedom to feasible solutions for the forward filter $\underline{\boldsymbol{R}}(\zeta)$ and thus may in practice be expected to yield less stationary noise enhancement and fewer problems resulting from possible ill-conditioning of the matrix $[\underline{\boldsymbol{\Phi}}(\zeta) \mid -\underline{\boldsymbol{U}}]$. On the other hand, any DFE can be susceptible to error propagation effects.

IV. Analysis—Minimum Mean-Square Error Equalization Expressions

Three expressions of the minimum mean square error (MMSE) of equalizers are considered. The three expressions are three of the four cases based on two types of equalizers in two types of interference environments, infinite-length continuous-time linear and decision-feedback equalizers, in stationary noise and cyclostationary interference. The model for cyclostationary interference signal is shown in Fig. 1(a) and as stated earlier is denoted by $\nu(t)$. The stationary noise model corresponds to the case where $\nu(t)$ is replaced by a wide-sense-stationary noise random process with same power spectral density. Define the three MMSEs to be ϵ_{lc}, ϵ_{ds}, and ϵ_{dc}; the subscripts l, d, s, and c, respectively denote *linear, decision-feedback, stationary noise*, and *cyclostationary interference*. Define $\Phi_i(f)$ to be the frequency responses (over unnormalized frequencies) corresponding the impulse responses $\phi_i(t)$ where $i \in \{0, 1, 2, \cdots, L\}$. When the frequency responses of these overall channels and cochannels are strictly bandlimited to $K/(2T)$ where K is a positive integer, then the MMSE expressions are [4]

$$\epsilon_{lc} = \left\langle \frac{1}{1 + M_c^T(f)} \right\rangle \tag{15}$$

$$\epsilon_{ds} = e^{-\langle \ln (1+M_s^T(f)) \rangle} \tag{16}$$

and

$$\epsilon_{dc} = e^{-\langle \ln (1+M_c^T(f)) \rangle} \tag{17}$$

where

$$\langle \bullet \rangle = T \int_{-1/(2T)}^{1/(2T)} (\bullet)\, df \tag{18}$$

$$M_s^T(f) = \frac{1}{T} \underline{\boldsymbol{\Phi}}_0^*(f) W_s^{-1}(f) \underline{\boldsymbol{\Phi}}_0(f) \tag{19}$$

$$M_c^T(f) = \frac{1}{T} \underline{\boldsymbol{\Phi}}_0^*(f) W_c^{-1}(f) \underline{\boldsymbol{\Phi}}_0(f) \tag{20}$$

$$W_s(f) = N_o \boldsymbol{I}_{2K-1} + \frac{1}{T} \sum_{i=1}^{L} \mathrm{diag}\, [\underline{\boldsymbol{\Phi}}_i(f) \underline{\boldsymbol{\Phi}}_i^*(f)] \tag{21}$$

$$W_c(f) = N_o \boldsymbol{I}_{2K-1} + \frac{1}{T} \sum_{i=1}^{L} \underline{\boldsymbol{\Phi}}_i(f) \underline{\boldsymbol{\Phi}}_i^*(f) \tag{22}$$

$$\underline{\boldsymbol{\Phi}}_i(f) = \left[\Phi_i\left(f - \frac{K-1}{T}\right), \cdots, \Phi_i\left(f - \frac{1}{T}\right), \Phi_i(f), \Phi_i\left(f + \frac{1}{T}\right), \cdots, \Phi_i\left(f + \frac{K-1}{T}\right) \right]^* \tag{23}$$

diag [$\bullet$] has the same diagonal elements as $\bullet$ with zeros off the main diagonal, $\boldsymbol{I}_{2K-1}$ is the identity matrix of order $2K-1$ and finally the symbol * denotes the complex conjugate transpose.

V. Performance Evaluations

A. Regions of suppressible ISI, ACI, and CCI

For the cases where the receiver and transmitter bandwidths are equal ($B_r = B_t$), $A_r = 1$ antenna, $N_c = 0$ CCI signals, the region where a generalized zero-forcing linear equalizer exists is determined using the analysis in Section III and plotted in Fig. 3; note that for clarity only the lower left boundary of the region is shown in the figure even though the region extends up to and beyond the upper right corner. Interestingly, there are operating points where increases in bandwidth pass in and out of regions where the generalized zero-forcing linear equalizer exists. The explanation is as follows. Under certain conditions, such as a change from a (C, B_t) point of (1.75, 1.0), which is in the feasible solution region to a point (1.75, 1.4), which is not, the increase in bandwidth causes more ACI than the linear equalizer is capable of suppressing. However, with a change from (1.75, 1.4) to (1.75, 1.6), it is true that there is more ACI, but more unknowns enter (9) for all frequencies, enough to equal the number of equations and hence provide a feasible solution. Curves for other values of receiver bandwidth equal to $2B_t$ and $3B_t$ are also shown in the figure, and as with the $1B_t$ case only the lower left boundary of the region is shown. Fig. 3 suggests that for arbitrary transmitter bandwidths increasing the receiver bandwidth allows for marginal improvements in spectral efficiency through decreased carrier spacing, but the carrier spacing canot be reduced below the normalized value of 1, which corresponds to an absolute carrier spacing value equal to the symbol rate. Note, however, that the ability to accommodate arbitrary transmitter bandwidths without necessarily sacrificing spectral efficiency allows increased system design flexibility; e.g. constant or nearly constant-envelope modulation may be allowed.

Fig. 4 is relevant to the case where $B_r = B_t$ with $N_c = 0$ CCI signals and the number of receiver antennas is varied. Increases in antenna diversity provide improvements in spectral efficiency below the $1/T$ limit associated with only increased receiver bandwidth, previously shown in Fig. 3. In an implementation, the gains associated with increases in antenna diversity would have diminishing returns [5], [6], [10].

Fig. 5 is relevant to the case where $B_r = 3B_t$ with $N_c = 1$ CCI signal and the number of antennas is varied. Even in the presence of one additional CCI signal, we find comparing with the $B_r = 3B_t$ curve in Fig. 3, that the combined benefits of increased diversity and relative bandwidth suggest operating points with spectral efficiencies comparable to the case with no additional CCI signals present.

The interference suppression capability of equalizers/combiners has three interpretations. It is a structure which can a) exploit the time-domain correlation in the interference [10], b) put nulls in the impulse responses of the equalized combined cochannels [11], or c) exploit the spectral correlation of the interference [3].

B. MMSE Results

The details of the system model need to be expanded further in order to evaluate the MMSE performance of the equalizers. An important note about the model and calculations to follow is that they are based on a non-fading channel. Thus, the calculations cannot be used to predict the exact performance in specific radio applications where fading exists. However, the positive aspect to this approach is that it applies to unfaded conditions and it is not tied to any specific application.

The cyclostationary ACI interference suppression capability of continuous-time infinite-length equalizers is analyzed under conditions with no CCI, one receiver antenna, and various conditions of transmitter and receiver bandwidth, and carrier spacing. The potential for performance improvements has implications on improved spectral effciency and the choice of system operating conditions.

The symbol rate $1/T$, the energy per symbol at the input to the equalizer E_S, and the noise power spectral density N_o are fixed. The energy per symbol at the input to the equalizer to the noise power spectral density is a constant, E_S/No, is arbitrarily set to

$$10\log_{10}\left(\frac{E_S}{N_o}\right) = 64.2 \text{ dB}. \tag{24}$$

The conditions of no CCI and one receiver antenna are specified as $N_c = 0$ CCI signals and $A_r = 1$ antenna. Since $N_c = 0$ CCI signals, L is even.

Expand the frequency response of the combined channel as

$$\Phi_0(f) = P_{t,0}(f)C_0(f)P_r(f) \tag{25}$$

and the frequency responses of the combined interferers as

$$\Phi_i(f) = P_{t,i}(f)C_i(f)P_r(f); \qquad i \in \mathcal{L}_1 \tag{26}$$

where $\{P_{t,i}(f)|i \in \mathcal{L}_0\}$ are the trnasmitter pulses, $C_0(f)$ is the frequency response of the channel, $\{C_i(f)|i \in \mathcal{L}_1\}$ are the frequency responses of the interferers, $P_r(f)$ is the frequency response of the receiver filter, and finally where

$$\mathcal{L}_0 = \{0, 1, 2, \cdots, L\} \tag{27}$$

$$\mathcal{L}_1 = \{1, 2, 3, \cdots, L\}. \tag{28}$$

The following is a commonly used pulse called a square-root raised cosine

$$P_{sr}(f;\, a) = \begin{cases} \sqrt{T}, & 0 \le |f| < \frac{1-a}{2T} \\ \sqrt{\frac{T}{2}\left(1 - \sin\left(\frac{\pi T}{a}\left(|f| - \frac{1}{2T}\right)\right)\right)}, & \frac{1-a}{2T} \le |f| < \frac{1+a}{2T} \\ 0, & \frac{1+a}{2T} \le |f| \end{cases}$$

$$0 \le a \le 1 \tag{29}$$

where a is the excess bandwidth parameter. However $P_{sr}(f;\, a)$ cannot have a bandwidth greater than $1/T$. To allow exploration of relatively wider bandwidths, the following pulse is *arbitrarily* defined

$$P_{srw}(f;\, B_t) = \begin{cases} \sqrt{E_S}P_{sr}(f;\, 2B_t - 1), & \frac{1}{2} \le B_t \le 1 \\ \sqrt{\frac{E_S}{B_t}}P_{sr}\left(\frac{f}{B_t};\, 1\right), & 1 < B_t \end{cases}. \tag{30}$$

The bandwidth of $P_{srw}(f;\, B_t)$ is B_t/T. When B_t is in the range $1/2 \le B_t \le 1$, $P_{srw}(f;\, B_t)$ behaves like a square-root raised cosine pulse. When B_t is in the range $1 < B_t$, $P_{srw}(f;\, B_t)$ has the same shape as a square-root raised cosine pulse with 100% excess bandwidth, but it is stretched linearly in frequency in order that the maximum bandwidth be B_t/T and the amplitude is scaled to maintain a constant transmitter power. Define

$$P_{t,i}(f) = P_{srw}\left(f - m_A[i]\frac{C}{T};\, B_t\right) \tag{31}$$

where $m_A[i]$ is any arbitrary one-to-one mapping from the number of the signal or interferer $\{i \in \mathcal{L}_0\}$ to its respective carrier frequency integer

$$m_A[i] \in \left\{-\frac{L}{2}, -\frac{L-2}{2}, \cdots, -2, -1, 0, 1, 2, \cdots, \frac{L-2}{2}, \frac{L}{2}\right\} \tag{32}$$

where L the number of ACI signals at the input to the equalizer is

$$L = 2\,\mathrm{int}\left(\frac{B_t + B_r}{C}\right). \tag{33}$$

The channel and ACI channels are ideal, i.e., no multipath or fading. However the wide transmitter pulses do introduce intersymbol interference. The frequency responses of the channels and ACI channels are

$$C_i(f) = e^{-j2\pi(D_i/T)(f - m_A[i])}; \qquad i \in \mathcal{L}_0 \tag{34}$$

where the dimensionless phase shifts (delays) of the channel and ACI channel signals relative to the symbol period are $\{D_i|i \in \mathcal{L}_0\}$; these values are arbitrarily set to zero.

The frequency response of the receiver filter is

$$P_r(f) = \begin{cases} \frac{1}{\sqrt{T}}P_{sr}(f;\, 2B_t - 1), & \frac{1}{2} \le B_t \le 1 \\ \frac{1}{\sqrt{T}}P_{sr}\left(\frac{f}{B_t};\, 1\right), & 1 < B_t. \end{cases} \tag{35}$$

It is based on the same pulse that is used for the transmitter, except the magnitude of the receiver frequency response is always unity at zero frequency.

Figs. 6 and 7 represent the two receiver bandwidth conditions $B_r = B_t$ and $B_r = 3B_t$, respectively. The case for $B_r = 2B_t$ is not shown because it does not introduce much new information. Each figure is a plot versus transmitter bandwidth and carrier spacing and contains two parts overlaid on each other. The parts are a contour plot of $10\log_{10}(\epsilon_{lc})$ and appropriate bandwidth curve from Fig. 3. These figures are overlaid for two reasons. The first is to allow a comparison between two major types of analyses, the existence of a generalized zero forcing linear equalizer and the MMSE of the linear equalizer. The second is to demonstrate the improvements in spectral efficiency that may be achieved by using wide receiver bandwidths. Inspection of Figs. 6 and 7 shows a very close agreement between the region where a generalized zero-forcing linear equalizer exists and where low MMSE values occur. The agreement is closer at the lower bandwidths in the figures. A change of the receiver bandwidth from $B_r = B_t$ to $B_r = 2B_t$ does not offer much improvement in spectral efficiency based on Fig. 3. However, a change from $B_r = 2B_t$ to $B_r = 3B_t$ offers a larger potential improvement in spectral efficiency. Such a move would allow lower carrier spacings than would be possible with no spectral overlap. Figs. 6 and 7 also suggest that for a linear equalizer with one receiver antenna, the carrier spacing cannot go below $1/T$ without tolerating residual ACI.

Figs. 8 and 9 are based on receiver bandwidths $B_r = B_t$ and $B_r = 3B_t$ symbol frequencies, respectively; they give the MMSE performance of a decision-feedback equalizer in cyclostationary interference, $10\log_{10}(\epsilon_{dc})$, for relatively narrow and wide receiver bandwidths. The lines of transitions from low-MMSE operating points to high-MMSE operating points moved to the left compared to the linear equalizer in Fig. 7. This move corresponds to improved performance. In Fig. 9, there are peaks in the surface, shown as concentric rings, on the conceptual line between the points (1, 1.5) and (2, 3). These peaks are operating points with very poor

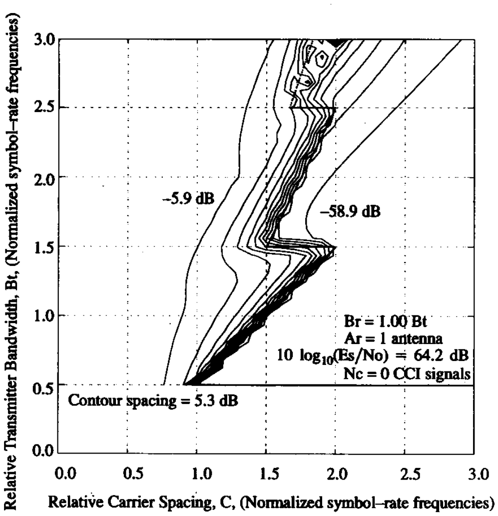

Fig. 6. Overlay of Fig. 3 with $10\log_{10}(\epsilon_{lc})$ MMSE surface versus transmitter bandwidth and carrier spacing—linear equalizer—cyclostationary interference—$B_r = B_t$.

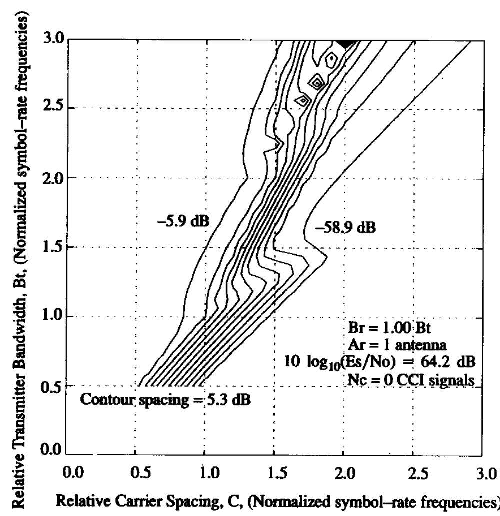

Fig. 8. $10\log_{10}(\epsilon_{dc})$ versus transmitter bandwidth and carrier spacing—decision-feedback equalizer—cyclostationary interference—$B_r = B_t$.

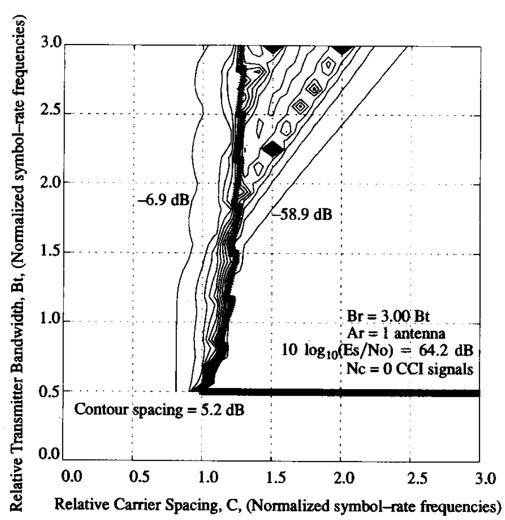

Fig. 7. Overlay of Fig. 3 with $10\log_{10}(\epsilon_{lc})$ MMSE surface versus transmitter bandwidth and carrier spacing—linear equalizer—cyclostationary interference—$B_r = 3B_t$.

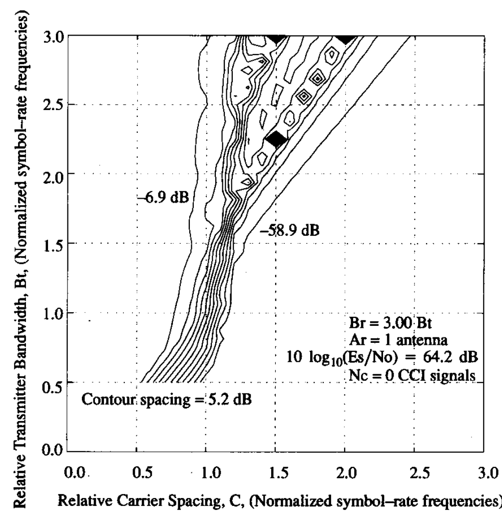

Fig. 9. $10\log_{10}(\epsilon_{dc})$ versus transmitter bandwidth and carrier spacing—decision-feedback equalizer—cyclostationary interference—$B_r = 3B_t$.

performance, i.e. high MMSE values. In the figures, as the transmitter bandwidths are increased with all other parameters fixed, it means that increasing numbers of ACI signals, (0, 2, 4, 6, $\cdots$), appear at the receiver input. The peaks occur directly on the transitions into operating regions where the number of additional ACI signals increases from 4 to 6. The difficulty experienced by the equalizer in achieving low MMSE values at these points occurs because in order to suppress ACI and ISI, the equalizer must synthesize frequency responses which cause noise enhancement.

For a decision-feedback equalizer with a bandwidth $B_r = 3B_t$, the performance differences between the cyclostationary interference and stationary noise cases are plotted in Fig. 10. It shows the gains available by exploiting the cyclostationarity of the ACI. Conceptually, the surface is composed of two hills in the upper right corner, surrounded by a plain in the lower right, lower left, and upper left corners. The hills are divided by a valley which runs along a line from the point (1, 1.5) to the point (2, 3). The lowest points on the surface are below the 4.3 dB contour on the plane around the hill. The highest point is on the top of the lower right plateau above the 47.3 dB contour. In the valley the interference is of a nature where it is very difficult for a decision-feedback equalizer to exploit the interference cyclostationarity. At the points (1.5, 2.25) and (2, 3) the surface has the values 4.1 dB and 3.1 dB, respectively. These points correspond to the worst peaks described in the previous paragraph. The valley and the two hills do not end in the upper right corner of Fig. 10. This suggests that the gains

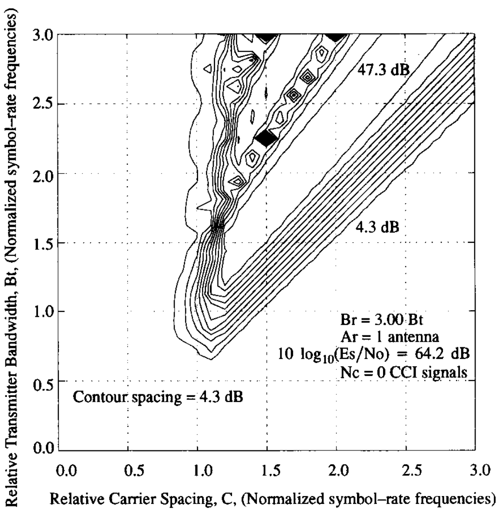

Fig. 10. Stationary-noise MMSE less cyclostationary-interference MMSE, $10\log_{10}(\epsilon_{ds}) - 10\log_{10}(\epsilon_{dc})$, versus transmitter bandwidth and carrier spacing—decision-feedback equalizer—$B_r = 3B_t$.

continue beyond what is shown in the upper right corner of the figure.

Regions of highest spectral efficiency lie around the smallest transmitter bandwidth, zero-percent excess bandwidth. It is shown that there are conditions where it is theoretically possible to operate at an infinite transmitter bandwidth and completely suppress all ISI, ACI, and CCI. More realistically, MMSE calculations incorporating the effects of noise show that under conditions of severe spectral overlap, linear and decision-feedback equalizers are able to provide significant interference suppression.

VI. Conclusion

Through the analysis of a generalized zero-forcing linear equalizer/combiner and decision-feedback equalizer, insight is offered about the ability of linear equalizers and linear combiners to suppress intersymbol, adjacent-channel, and cochannel interference. This analysis provided the following results, of which only the first result had the additional confirmation through calculations in the digital radio application.

1) With one antenna and a linear equalizer, arbitrarily large receiver bandwidths allow for marginal improvements in spectral efficiency through decreased carrier spacing, but the carrier spacing cannot go below the fundamental carrier spacing value equal to the symbol rate without likely tolerating residual interference.
2) The use of equalizers and linear combiners, together with large receiver bandwidths, allows large transmitter bandwidths to be used. This may allow system design flexibility; e.g. constant or near-constant envelope modulation.
3) Large receiver bandwidths assist multiple antennas in improving the spectral efficiency in that carrier spacing values may go below the symbol rate, even in the presence of CCI.
4) For CCI and ISI, the number of interferers that may be suppressible by a generalized zero-forcing linear equalizer/combiner increases linearly with the product of the number of antennas and the truncated integer ratio of the total bandwidth to the symbol rate.

A comparison to the first result using calculations of minimum mean square equalizer performance is made for one receiver antenna and no cochannel interferers. These results demonstrated how equalizers are able to extract the signal of interest and to provide interference suppression even under conditions of considerable mutual overlaps of all signals. Greater interference suppression is possible using equalizers with larger receiver bandwidths. The larger receiver bandwidths enhance the differences between combined channel and combined interferers to offer the equalizers a greater opportunity for interference suppression. For the case of one antenna, agreement is confirmed between the minimum mean square error calculations and the generalized zero-forcing linear equalizer analyses to predict good system operating points. For the case of multiple antennas, this increases confidence in other predictions from the generalized zero-forcing linear equalizer analysis. Note that the linear and decision feedback equalizers discussed here are of conventional design, and would be adapted using LMS or other algorithms based on minimizing the mean square error. The equalizer's input sampling rate would of course have to be twice the receiver's bandwidth.

Acknowledgment

The authors thank the reviewers for their help in improving the document.

References

[1] D. C. Cox, "Cochannel interference considerations in frequency reuse small-coverage-area radio systems," *IEEE Trans. Commun.*, vol. COM-30, pp. 135–142, Jan. 1982.

[2] S. Wang and S. S. Rappaport, "Signal-to-interference calculations for balanced channel assignment patterns in cellular communications," *IEEE Trans. Commun.*, vol. 37, pp. 1077–1087, Oct. 1989.

[3] W. A. Gardner, "Exploitation of spectral redundancy in cyclostationary signals," *IEEE Signal Processing Mag.*, vol. 8, pp. 14–36, Apr. 1991.

[4] B. R. Petersen and D. D. Falconer, "Minimum mean-square equalization in cyclostationary and stationary interference-analysis and subscriber-line calculations," *IEEE J. Select. Areas Commun.*, vol. 9, pp. 931–941, Aug. 1991.

[5] P. Monsen, "MMSE equalization of interference on fading diversity channels," *IEEE Trans. Commun.*, vol. COM-32, pp. 5–12, Jan. 1984.

[6] J. H. Winters, "Optimum combining in digital mobile radio with cochannel interference," *IEEE J. Select. Areas Commun.*, vol. SAC-2, pp. 528–539, July 1984.

[7] N. Kinoshita and S. Sampei, "Method of rejecting adjacent channel interference using an adaptive equalizer," *Electron. Commun. Japan, Part I: Commun.*, vol. 72, no. 11, pp. 1–10, Oct. 1989.

[8] P. Niger and P. Vandamme, "Performance of equalization techniques in a radio environment," *IEEE Trans. Commun.*, vol. 39, pp. 452–457, Mar. 1991.

[9] S. K. Wilson and J. M. Cioffi, "Multi-dimensional equalization for adjacent-channel interference," in *Conf. Rec. IEEE ICC 91*, Denver, CO, June 23–26, 1991, vol. 3, pp. 1398–1402.

[10] C. L. Despins, D. D. Falconer, and S. A. Mahmoud, "Compound strategies of coding, equalization, and space diversity for wideband TDMA indoor wireless channels," *IEEE Trans. Vehic. Technol.*, to be published.

[11] D. A. Shnidman, "A generalized Nyquist criterion and an optimum linear receiver for a pulse modulation system," *Bell Syst. Tech. J.*, vol. 46, no. 9, pp. 2163–2177, Nov. 1967.

Brent R. Petersen (S'85–M'92) was born in Whitehorse, Yukon Territory, Canada, on March 25, 1962. He received the B.Eng. degree in electrical engineering from Carleton University, Ont., Canada, in 1985 and the M.A.Sc. degree in electrical engineering from the University of Waterloo, Ont., Canada, in 1987. He returned to Carleton University where he received the Ph.D. degree in electrical engineering in 1992.

He held a postdoctoral fellowship at the IBM Zurich Research Laboratory where his main responsibility was research in wireless communication, which included participation in the EC-funded RACE project. His research interests have been in digital communications, digital signal processing, and computer-aided design of integrated circuits.

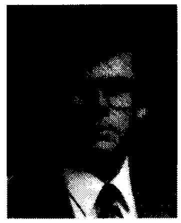

David D. Falconer (M'68–SM'83–F'86) was born in Moose Jaw, Sask., Canada, on August 15, 1940. He received the B.A. Sc. degree in engineering physics from the University of Toronto in 1962, and the S.M. and Ph.D. degrees in electrical engineering from M.I.T., Cambridge, in 1963 and 1967, respectively.

After a year as a postdoctoral fellow at the Royal Institute of Technology, Stockholm, Sweden he was with Bell Laboratories, Holmdel, NJ, from 1967 to 1980, as a Member of Technical Staff and later as group supervisor. During 1976–1977 he was a visiting professor at Linköping University, Linköping, Sweden. Since 1980 he has been at Carleton University, Ottawa, Ont., Canada, where he is a Professor in the Department of Systems and Computer Engineering. His interests are in digital communications, signal processing, and communication theory.

Dr. Falconer was Editor for Digital Communications for the IEEE TRANSACTIONS ON COMMUNICATIONS from 1981 to 1987. He is a member of the Association of Professional Engineers of Ontario. He was awarded the Communications Society Prize Paper Award in Communications Circuits and Techniques in 1983 and in 1986. He was a consultant to Bell-Northern Research in 1986–1987 and to Codex/Motorola in 1990–1991, during sabbaticals.